Structure and phospholipase function of peroxiredoxin 6: identification of the catalytic triad and its role in phospholipid substrate binding[1]

Yefim Manevich,[*] Konda S. Reddy,[†] Tea Shuvaeva,[*] Sheldon I. Feinstein,[*] and Aron B. Fisher[2,*]

Institute for Environmental Medicine* and Department of Biochemistry and Biophysics,† University of Pennsylvania Medical Center, Philadelphia, PA 19104

Abstract **Peroxiredoxin 6 (Prdx6) is a bifunctional protein with glutathione peroxidase and phospholipase A_2 (PLA_2) activities, and it alone among mammalian peroxiredoxins can hydrolyze phospholipids. After identifying a potential catalytic triad (S32, H26, D140) from the crystal structure, site-specific mutations were used to evaluate the role of these residues in protein structure and function. The S32A mutation increased Prdx6 α-helical content, whereas secondary structure was unchanged by mutation to H26A and D140A. Lipid binding by wild-type Prdx6 to negatively charged unilamellar liposomes showed an apparent rate constant of $11.2 \times 10^6\ M^{-1}\ s^{-1}$ and a dissociation constant of 0.36 μM. Both binding and PLA_2 activity were abolished in S32A and H26A; in D140A, activity was abolished but binding was unaffected. Overoxidation of the peroxidatic C47 had no effect on lipid binding or PLA_2 activity. Fluorescence resonance energy transfer from endogenous tryptophanyls to lipid probes showed binding of the phospholipid polar head in close proximity to S32. Thus, H26 is a site for interfacial binding to the liposomal surface, S32 has a key role in maintaining Prdx6 structure and for phospholipid substrate binding, and D140 is involved in catalysis. This putative catalytic triad plays an essential role for interactions of Prdx6 with phospholipid substrate to optimize the protein-substrate complex for hydrolysis.**—Manevich, Y., K. S. Reddy, T. Shuvaeva, S. I. Feinstein, and A. B. Fisher. **Structure and phospholipase function of peroxiredoxin 6: identification of the catalytic triad and its role in phospholipid substrate binding.** ***J. Lipid Res.*** **2007.** 48: **2306–2318.**

Supplementary key words liposomes • circular dichroism • fluorescence resonance energy transfer • site-directed mutagenesis • lipid binding • peroxidase

Peroxiredoxins are a superfamily of nonheme and nonselenium peroxidases that are widely distributed throughout all phyla (1). All six mammalian peroxiredoxins have peroxidase activity in which the peroxidatic cysteine is oxidized to a sulfenic acid by the peroxide substrate (2). In 2-cys peroxiredoxins, the peroxidized (catalytic) cysteine and a second surface-associated (resolving) cysteine interact to form a disulfide; the disulfide is reduced back to the sulfhydryl by thioredoxin to complete the catalytic cycle (3). However, in peroxiredoxin 6 (Prdx6), also called 1-cys peroxiredoxin and antioxidant protein 2, the single conserved cysteine (Cys47) is buried inside the protein globule. In this enzyme, the catalytic cysteine after oxidation is reduced by glutathione S-transferase-bound GSH to complete the catalytic cycle (4). Prdx6 also has a second catalytic activity, namely phospholipase A_2 (PLA_2), that is Ca^{2+}-independent, maximal at pH 4, and has a major role in the metabolism of the phospholipids of lung surfactant (5). The PLA_2 activity of Prdx6 is inhibitable by "serine protease" inhibitors, providing evidence for a serine as the active center (6–8). The primary sequence of Prdx6 at amino acids 30–34 indicates a "lipase" motif (GXSXG), which occurs in essentially all serine-dependent lipases (9). This motif is not present in other peroxiredoxins (10). Furthermore, examination of the crystal structure of Prdx6 (11) suggests that S32 is part of a surface-localized catalytic triad (S32, H26, D140) that is common for serine-based PLA_2 (9, 12) (**Fig. 1**). Site-directed mutation of S32 resulted in the loss of PLA_2 activity, which was interpreted to confirm a role for this amino acid moiety in catalysis (13).

Manuscript received 6 October 2006 and in revised form 29 June 2007.

Published, JLR Papers in Press, July 24, 2007.
DOI 10.1194/jlr.M700299-JLR200

Abbreviations: bisPyr-PC, 1,2-bis(1-pyrenedecanoyl)-*sn*-glycero-phosphocholine; CD, circular dichroism; DPPC, dipalmitoyl phosphatidylcholine; FRET, fluorescence resonance energy transfer; [^{3}H]DPPC, 1-palmitoyl,[9,10-^{3}H]2-palmitoyl *sn*-glycero-3-phosphocholine; MJ33, 1-hexadecyl-3-trifluoroethyl-*sn*-glycero-2-phosphomethanol; N-DNS-PE, *N*-(5-dimethylaminonaphthalene-1-sulfonyl)-*sn*-glycero-3-phosphoethanolamine; PC, phosphatidylcholine; PE, phosphatidylethanolamine; PG, phosphatidylglycerol; PLA_2, phospholipase A_2; PLPC, 1-palmitoyl,2-linolenoyl-*sn*-glycero-3-phosphatidylcholine; Prdx6, peroxiredoxin 6; PS, phosphatidylserine; 2Pyr-PC, 1-hexadecanoyl-2-(1-pyrenedecanoyl)-*sn*-glycero-3-phosphocholine.

[1] This work was presented in part at the Experimental Biology meetings in April 2004 (Washington, DC) and April 2005 (San Diego, CA).

[2] To whom correspondence should be addressed.
e-mail: abf@mail.med.upenn.edu

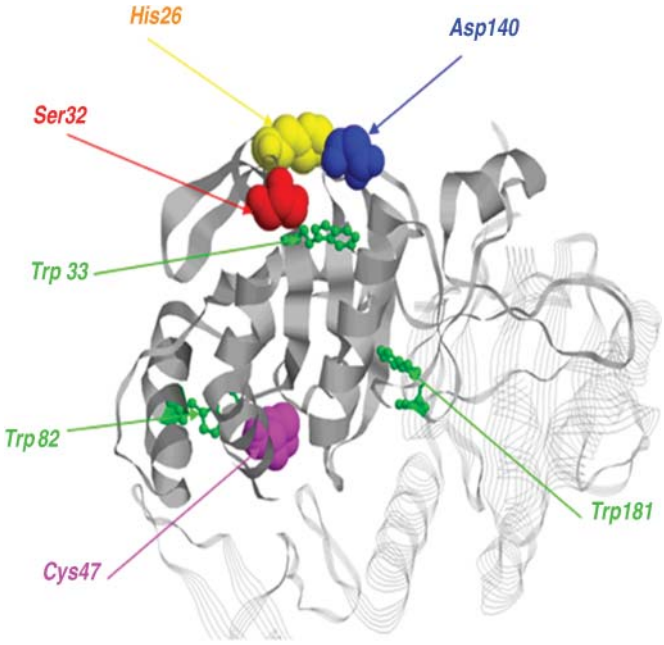

Fig. 1. Model of peroxiredoxin 6 (Prdx6) structure. The model is based on the published crystal structure [Protein Data Bank number 1PRX (11)]. Positions are shown for tryptophan 33, 82, and 181 (green), serine 32 (red), histidine 26 (yellow), aspartate 140 (blue), and oxidized cysteine 47 (purple). S32, H26, and D140 form a phospholipase A_2 (PLA_2) catalytic triad, and C47 is the catalytic center for peroxidase activity. One monomer of the Prdx6 homodimer is represented as a ribbon model (gray), and another monomer is represented as a strand model.

The PLA_2 activity of Prdx6 showed broad specificity toward phospholipids, although activity was greatest with phosphatidylcholine (PC) as the substrate (7). Apparent kinetic constants for PLA_2 activity of bovine Prdx6 with dipalmitoyl phosphatidylcholine (DPPC) substrate in unilamellar liposomes with a composition [50% DPPC, 25% egg PC, 15% cholesterol, and 10% phosphatidylglycerol (PG)] that mimics that of lung surfactant were K_m = 0.35 mM and V_{max} = 70 nmol/min/mg protein (7). Activity with alkyl ether PC was decreased by ~60% compared with DPPC, whereas lysophospholipase, PLA_1, and platelet activation factor acetylhydrolase activities were not detected (6, 7). Competitive inhibition of Prdx6 PLA_2 activity by the transition state analog 1-hexadecyl-3-trifluoroethyl-*sn*-glycero-2-phosphomethanol (MJ33) was shown in vitro with recombinant protein (13), ex vivo in lysate from isolated granular pneumocytes (14), and in homogenate of rat lung (15, 16).

Although the Prdx6-mediated hydrolysis of phospholipids has been well documented (6–8, 13), the functional importance of specific amino acid residues in substrate binding to enzyme and in catalysis is not known. Furthermore, phospholipid substrate binding and orientation relative to the Prdx6 binding site is important in the understanding of the enzyme's conformational dynamics, which may result in synergy or independence of the PLA_2 and peroxidase activities. The present study of this bifunctional enzyme is focused on its specific binding of phospholipid substrate at pH 4, which is optimal for its PLA_2 activity (6, 7, 13). We used fluorescently labeled unilamellar liposomes to evaluate the kinetics of binding of the enzyme to the interface in real time, the positioning of the phospholipid substrate upon binding, and the effects of substrate binding and site-specific mutations on protein secondary structure to understand the mechanism for PLA_2 activity. Mutagenesis of S32, H26, and D140 was used to evaluate the role of the putative catalytic triad in protein function, whereas mutagenesis of the protein tryptophanyls W33 and W82 was used to confirm their role as natural reporter fluorophores (Fig. 1).

EXPERIMENTAL PROCEDURES

Materials

DPPC, 1-palmitoyl,2-linolenoyl-*sn*-glycero-3-phosphatidylcholine (PLPC), egg PC, PG, phosphatidylserine (PS), and cholesterol were purchased from Avanti Polar Lipids (Birmingham, AL). 1-Palmitoyl,[9,10-^{3}H]2-palmitoyl *sn*-glycero-3-phosphocholine ([^{3}H]DPPC) was purchased from Perkin-Elmer Life Science (Boston, MA). *N*-(5-Dimethylaminonaphthalene-1-sulfonyl)-1,2-dihexadecanoyl-*sn*-glycero-3-phosphoethanolamine (N-DNS-PE), 1-hexadecanoyl-2-(1-pyrenedecanoyl)-*sn*-glycero-3-phosphocholine (2Pyr-PC), and 1,2-bis(1-pyrenedecanoyl)-*sn*-glycero-3-phosphocholine (bisPyr-PC) were purchased from Molecular Probes (Eugene, OR). MJ33 and all other reagents were purchased from Sigma (St. Louis, MO).

Generation of recombinant rat wild-type and mutant Prdx6

The cloning of rat Prdx6 cDNA (8) and its expression construct (4) in pETBlue-1 (Novagen, Madison, WI) have been described previously. Mutagenesis was performed using the QuikChange site-directed mutagenesis kit (Stratagene, La Jolla, CA), according to the manufacturer's instructions. Complementary mutagenic oligonucleotide pairs were purchased from Qiagen Operon (Valencia, CA), one to prime the synthesis of each strand. The mutagenic substitutions in each oligonucleotide are represented by the underlined letters within the oligonucleotide sequences below.

For the S32A mutation, the oligonucleotide primers were 5′-CACGATTTCCTAGGAGATGCATGGGGCATTCTCTTTTCC-3′ (forward) and 5′-GGAAAAGAGAATGCCCCATGCATCTCCTAG-GAAATCGTG-3′ (reverse). For the H26A mutation, the oligonucleotide primers were 5′-CGGCCACATCCGTTCCGCCGATTTCC-TAGGAGATTC-3′ (forward) and 5′-GAATCTCCTAGGAAATCG-GCGAAGCGGATGTGGCCG-3′ (reverse). For the D140A mutation, the oligonucleotide primers were 5′-GTGGTATTCATTTTTGGCC-CTGCCAAGAAACTAAAACTGTCCATCC-3′ (forward) and 5′-GGA-TGGACAGTTTTAGTTTCTTGGCAGGGCCAAAAATGAATAC-CAC-3′ (reverse). The oligonucleotides used to generate the W33F mutation were 5′-CCACGATTTCCTAGGAGATTCATTTGG-CATTCTCTTTTCCC-3′ (forward) and 5′-GGGAAAAGAGAATGC-CAAATGAATCTCCTAGGAAATCGTGG-3′ (reverse). For the W82F mutation, the oligonucleotide primers were 5′-GTTGAGGACCATT-TTGCCTTTAGCAAGGACATCAATGCTTAC-3′ (forward) and 5′-GTAAGCATTGATGTCCTTGCTAAAGGCAAAATGGTCCTC-AAC-3′ (reverse).

The rat Prdx6 pET-Blue-1 expression plasmid (5–50 ng) was denatured and annealed with 100 ng/μl of each mutagenic oligonucleotide primer in a thermal cycler in the presence of 2.5 units of Pfu Turbo polymerase. After 18 cycles (for the aspartate-

to-alanine mutations), 16 cycles (for the tryptophan-to-phenylalanine mutations), or 12 cycles (for the serine- or histidine-to-alanine mutations), the reaction was stopped by placing it on ice for 2 min, then treated with 10 units of the restriction enzyme *Dpn*I for 1 h at 37°C to digest the parental DNA (methylated and unmutated); 1 μl of each reaction was then used to transform into supercompetent *Escherichia coli* XL-1-Blue cells. After allowing cells to recover for 1 h at 37° in a shaker-incubator, they were placed on plates containing ampicillin (for selection) and incubated overnight until colonies appeared. Colonies were screened by oligonucleotide sequencing of the entire Prdx6 coding region (University of Pennsylvania Cell Center), and those found to have only the desired mutation were transformed into Tuner (DE3) pLacI cells (Novagen). Prdx6 DNA containing the D140A mutation was cloned between the *Bgl*II and *Spe*I sites of the polylinker in the insect cell vector, pMT/BiP/V5-His (Invitrogen, Carlsbad, CA). Subsequently, *Drosophila* S2 cells were cotransfected with pMT/BiP/V5-His plasmid and pCoBlast (Invitrogen) at a 19:1 weight ratio, and stable transfectants were established by adding blasticidin (25 μg/ml). Prdx6 was secreted into the medium of the S2 cells.

Proteins were purified as described previously (4) or, for the D140A mutation, using immunoaffinity chromatography with a polyclonal antibody to the recombinant wild-type human protein. The identities of isolated proteins were confirmed by SDS-PAGE and Western blot (data not shown), which revealed a homogeneous product. Analysis of the wild-type protein by size exclusion HPLC (YMC-10, 500 × 8 mm inner diameter, 120 Å pore; Waters, Milford, MA) using 0.5 ml/min isocratic elution with 0.15 M NaCl in 0.1 M PBS, pH 7.0, showed two major peaks corresponding to the Prdx6 monomer and homodimer, as reported previously (4). Similar results showing two peaks were obtained with the H26A, D140A, W33F, and W82F mutants, but the S32A mutant showed a single peak (data not shown) compatible with the monomer.

Liposome preparation

Unilamellar liposomes consisting of DPPC/egg PC/cholesterol/PG (50:25:15:10, mol/mol) were prepared by extrusion under pressure, as described previously (15). Liposomes also were prepared by replacing PG with an equivalent amount of phosphatidylethanolamine (PE) or phosphatidylserine (PS). Fluorescently labeled liposomes were prepared by replacing 2 mol% of egg PC with N-DNS-PE or bisPyr-PC probes. The sizes of the liposome particles were analyzed by dynamic light scattering (DLS 90 Plus Particle Size Analyzer; Brookhaven Instruments, Holtsville, NY) before and after Prdx6 addition. The analysis showed a homogeneous population of liposomes with a diameter of ~100–120 nm, which represented >95% of total vesicles and showed relatively little change with the addition of Prdx6 (**Table 1**).

Fluorescence measurements

The fluorescently labeled phospholipids N-DNS-PE and bisPyr-PC or 2Pyr-PC were used to study the interaction of phospholipids and Prdx6. The selection of the probes was based on the polar head localization of the DNS chromophore and the ω-position of the pyrene chromophore in the *sn*-2-acyl chain. Because of the high sensitivity of pyrene probes to O_2-induced quenching (17), the buffers used for fluorescence studies were bubbled with N_2 for 45 min at 4°C. All fluorescence studies were done at 22 ± 0.5°C using a temperature-controlled water circulator. Fluorescence was measured with a Photon Technology International, Inc. (Lawrenceville, NJ), spectrofluorometer equipped with a single photon counting system for fluorescence intensity detection, dual fluorescence and absorbance channels, and a water bath temperature-controlled sample holder using excitation and emission slits of 1 and 2 nm, respectively.

Calculation of the rate constant and dissociation constant for binding of Prdx6 to liposomes

For studies of binding, Prdx6 was treated with a 4× molar excess of H_2O_2 for 1 h at room temperature to oxidize the peroxidatic C47 and thereby inactivate the peroxidase activity. Matrix-assisted laser-desorption ionization time of flight mass spectrometry analysis of protein showed an increase of molecular mass from 24,687 to 24,721 (Δ 34 Da), compatible with oxidation of the cysteine to the cysteine sulfinic acid. Subsequent studies presented below indicate that this overoxidation of Prdx6 has no effect on either its binding of phospholipids or its PLA_2 activity at pH 4.

Real-time determination of the binding of Prdx6 proteins (3.2 μM final concentration) to unilamellar liposomes (100 μM total phospholipid in 40 mM Na acetate buffer, pH 4.0) was done in the time-based ratiometric mode of the fluorometer, with recording of one measurement per second for 15 min before and 45 min after the addition of protein. Measurements were made at 415/505 nm for N-DNS-PE or 382/470 nm for bisPyr-PC, with constant stirring of the sample before and after the addition of protein. The experimental data were approximated with the use of the standard sigmoid fit (four parameters) using SigmaPlot 2001, version 7.0 (SPSS, Chicago, IL). R^2 for all fits was >0.98.

The calculation of binding constants assumes that the value of the fluorescence intensities ratio (R; 415/505 nm or 382/470 nm) represents the amount of Prdx6 that is bound to the surface of liposomes under the conditions of the experiment. Because Prdx6 used in our binding studies is catalytically inactive,

TABLE 1. Dynamic light-scattering analysis of N-DNS-PE-labeled unilamellar liposomes

N-DNS-PE-Labeled Liposome[a]	Diameter		Population from Total	
	Before Prdx6 Addition	After Prdx6 Addition	Before Prdx6 Addition	After Prdx6 Addition
	nm	*nm*	%	%
PG	103 ± 0.880	108 ± 0.895	97	97
PS	104 ± 0.877	105 ± 0.868	94	94
PE	122 ± 0.833	124 ± 0.896	100	100

DPPC, dipalmitoyl phosphatidylcholine; N-DNS-PE, *N*-(5-dimethylaminonaphthalene-1-sulfonyl)-*sn*-glycero-3-phosphoethanolamine; PE, phosphatidylethanolamine; PG, phosphatidylglycerol; PS, phosphatidylserine. Data represent means ± SEM for 20 independent experiments. Incubation was at pH 4 for 1 h as described in Experimental Procedures for phospholipase A_2 assay.

[a] Liposomes contained 10% of the indicated phospholipid plus 50% dipalmitoyl phosphatidylcholine, 25% egg phosphatidylcholine, and 15% cholesterol.

the scheme for binding is: E + S ⇆ ES. The linear portion of the curves for Prdx6 binding to liposomes versus time represents only ES formation, and we assume that under this condition the forward reaction is much greater than the reverse reaction. This linear rate was used to calculate d[ES]/dt and then the rate constant (k_1) for binding. The value for k_1 is calculated from $d[ES]/dt = k_1[E][S]$, where [E] is the starting concentration of Prdx6, [S] is the starting concentration of lipids in the outer leaf of the liposome, and [ES] is the concentration of the Prdx6-liposome complex. Saturation of the kinetic curve ($d[ES]/dt = 0$), indicated by maximal fluorescence intensity, represents maximal enzyme bound to liposomes. This value was used to calibrate the fluorescence output to determine [ES]. The maximal amount (in molecules) of Prdx6 bound per unilamellar liposome (50 nm radius) is calculated from: $S/S_p = 4\pi r_l^2/\pi r_P^2 = 1{,}600$, where S is the liposome surface area, S_P is the Prdx6 monomer cross-sectional area, r_l is the radius of the liposome, and r_P is the radius of the Prdx6 monomer. The Stokes radius for the Prdx6 monomer was determined by HPLC size exclusion chromatography (4, 18) as 25 Å. Assuming that the surface area of a phospholipid molecule is 63 $Å^2$ (19), a liposome of 100 nm diameter (Table 1) would contain $\sim 10^5$ mol of phospholipid. Thus, there are 1.8×10^{12} liposomes in the cuvette (3 ml volume, 100 μM phospholipid) during the fluorescence experiment. To fully occupy the liposome surface with protein at saturation would require 1.6 μM Prdx6. Because $\sim 5 \times 10^4$ phospholipid molecules (half of the total) are present in the outer leaflet, there would be ~31 molecules of phospholipid per molecule of Prdx6 at saturation. We used 3.2 μM Prdx6 in these studies to provide an excess of protein, and 8 or 16 μM Prdx6 had no greater effect on the calculated kinetic parameters (data not shown).

To determine the dissociation constant (K_d), the maximal fluorescence ratio (R_{max}; 415/505 nm) was recorded for varying concentrations of Prdx6 (0–16 μM) in the presence of 100 μM N-DNS-PE-labeled liposomes. The R_{max} value was plotted versus concentration of Prdx6, and 50% of the saturating value was calculated as the apparent K_d for enzyme binding to liposomes. To validate the equilibrium between bound and free Prdx6 using fluorescence detection, N-DNS-PE-labeled (2 mol%) liposomes (100 μM) were incubated with 3.2 μM Prdx6 for 30 min at room temperature. The solution in 40 mM Na acetate (pH 4.0) was loaded onto a YM-100 (100 kDa cutoff) Centricon centrifugal filter device (Millipore, Bedford, MA) and centrifuged at 2,000 *g* for 20 min at 4°C. The filtrate and retentate were collected and analyzed for protein concentration and for protein and DNS fluorescence and by SDS-PAGE and Western blot for Prdx6.

Positioning of substrate upon binding to Prdx6

Prdx6 contains three tryptophan residues (W33, W82, and W181). Because W33 is adjacent to S32 and W82 is only ~3.5 Å away from C47 (Fig. 1), these amino acids were used as natural fluorescent labels in Prdx6 to study the position of the phospholipid substrate upon its binding. Tryptophanyl fluorescence (0.5 μM Prdx6 in 40 mM Na acetate, pH 4.0, 22°C in a quartz cuvette) was recorded with excitation at 295 nm to minimize the input of phenylalanine and tyrosine residues. Appropriate controls were subtracted from the final spectra. Micellar suspensions of the fluorescent lipid probes were used for fluorescence resonance energy transfer (FRET) analysis of the interaction between Prdx6 and lipids. FRET from Prdx6 tryptophanyls to N-DNS-PE and the bisPyr-PC or 2Pyr-PC probe was measured to determine the position of the phospholipid polar head and acyl chain, respectively. These probes provided sufficient overlap between tryptophanyl fluorescence of the protein and the DNS and pyrene chromophore absorbance spectra and had similar relatively small Förster radii (21–24 Å) for the tryptophan-DNS and tryptophan-Pyr couples (20). Micellar suspensions of the probe were prepared by injection of an ethanol solution (with the addition of ~1% chloroform) of bisPyr-PC, 2PyrPC, or N-DNS-PE (10 mM) into 40 mM Na acetate buffer (pH 4), to give a final probe concentration of ~0.1 μM. Analysis of probe solutions using a static light-scattering instrument with resolution approaching 1 nm (BI-200 SM; Brookhaven Instruments) failed to demonstrate the presence of particles, and absorbance for the solution at 340 nm was <0.1 optical density units. To study FRET from protein tryptophanyls to pyrene chromophores, various concentrations of Prdx6 or mutant proteins were added to micellar solutions containing the probes. The fluorescence of protein and the Pyr- and DNS-labeled phospholipid mixture was measured with excitation at 295 nm for the detection of probe effects on protein fluorescence. To compensate for different emission intensities associated with mutation of the protein tryptophans, FRET spectra were normalized for the maximal emission of protein in the absence of probe.

Enzymatic activity assay

PLA_2 activity was measured as described previously (5) using [^{3}H]DPPC in liposomes as substrate in 40 mM Na acetate buffer, pH 4.0, that also contained 5 mM EDTA and 1 mM glutathione. Trace [^{3}H]DPPC was added to the standard mixture of lipids to give a specific activity of ~4,500 dpm/nmol. Protein concentration was measured using the Bradford Protein Assay (Bio-Rad, Hercules, CA).

Circular dichroism measurement

Circular dichroism (CD) measurements were carried out with 202 and 62 DS spectrometers (AVIV Associates, Lakewood, NJ) using a semimicro quartz rectangular 1 × 10 × 40 mm cuvette. The protein samples (10 μM in 40 mM Na acetate, pH 4.0 buffer) were maintained at 20°C using a Pelletier element. Spectra were recorded while scanning in the far-ultraviolet region (190–260 nm), with bandwidth of 1.0 nm, step size of 0.2 nm, integration time of 30 s, and with three repeats. Melting curves were recorded at 220 nm from 10°C to 90°C at increments of 0.5°C. The output of the CD spectrometer was recalculated according to the protein concentration, amino acid content, and cuvette thickness into molecular ellipticity units (degrees/cm^2/dmol). The melting point is the temperature at 50% loss of molecular ellipticity. Percentages of α-helices, β-strands, and random structures in the protein secondary structure were calculated from the CD spectra using K_{2d} (www.embl-heidelberg.de/-andrade/k2d.html) (21). The direct comparison of secondary structure predicted by K_{2d} showed good agreement with the known secondary structure of oxidized Prdx6.

TABLE 2. PLA_2 activity of Prdx6 wild-type and mutant proteins

Protein	PLA_2 Activity
	nmol/min/mg protein
Wild type	105 ± 1.7
Oxidized wild type	107 ± 2.7
S32A	0.4 ± 0.05
H26A	0.6 ± 0.2
D140A	2.9 ± 0.6
W33F	53.9 ± 3.4
W82F	101 ± 0.7

Activity was measured at pH 4.0 in buffer containing 40 mM Na acetate, 5 mM EDTA, and 1 mM GSH. Values are means ± range (n = 2) except for the wild-type protein, which is mean ± SEM (n = 4).

Immunoblot analysis

SDS-PAGE (12% Tris-glycine) used the Nu-PAGE system (Invitrogen) with loading of ~2 μg of protein per lane. After electrophoretic resolution, the proteins were electroblotted to Immobilon-P membranes (Millipore) using a Trans-Blot® SD Semi-Dry Transfer Cell (Bio-Rad) at 10 V for 30 min. Membranes were probed with a monoclonal anti-Prdx6 antibody (8) at a dilution of 1:1,400 in blocking buffer. Blots were developed using anti-mouse IRDye™ 800DX (green) secondary antibody (Rockland, Gilbertsville, PA) according to the manufacturer's instructions and were analyzed with the Odyssey Dual-Color Infrared Excited Imaging System (Li-Cor, Lincoln, NE).

RESULTS

Effects of mutations on Prdx6 PLA_2 activity

The PLA_2 activity of wild-type and mutant Prdx6 proteins was measured by radiochemical assay with [^{3}H]DPPC in mixed unilamellar liposomes as substrate (**Table 2**). The activity of wild-type recombinant rat Prdx6 was similar to our previously reported value for recombinant histidine-tagged human protein (21) and was ~50% greater than the reported value for native protein isolated from bovine lung (7). This higher level of activity was associated with the presence of GSH in the assay buffer, although the mechanism for this effect is not known. Overoxidation of C47 to sulfinic acid abolished peroxidase activity (data not shown) but had no effect on PLA_2 activity (Table 2), similar to the C47S mutation as described previously (13). As in our previous report (13), the S32 mutation abolished PLA_2 activity (Table 2). The H26A and D140A mutations also abolished PLA_2 activity, whereas the W33F mutation resulted in a decrease in activity by ~50%; the W82F mutation had no effect on activity (Table 2).

Prdx6 binding to unilamellar liposomes

The N-DNS-PE probe was used to label the surface of liposomes, and peroxiredoxin binding to liposomes was studied by recording real-time changes in the 415/505 nm fluorescence ratio. Shift of the fluorescence maximum of DNS in liposomes from 505 to 415 nm in the presence of Prdx6 reflects a change in the polarity of its surroundings (17) attributable to shielding of the DNS chromophore by bound protein. Thus, the increases in fluorescence ratio indicate binding of Prdx6 to the liposomal surface. Prdx6 binding to the liposomal surface also is shown by the increase of pyrene monomer fluorescence (382 and ~393 nm maxima) at the expense of pyrene excimer fluorescence (470 nm maximum), compatible with increased separation of the pyrene-labeled acyl chains (**Fig. 2B**). The increase in the ratio of fluorescence at 415/505 nm for N-DNS-PE and at 382/470 nm for bisPyr-PC associated with Prdx6 binding is independent of the actual fluorescent probe concentration in liposomes. Preincubation of Prdx6 with equimolar MJ33 before its addition to liposomes substantially inhibited protein binding (data not shown). MJ33 is a transition state analog that is a competitive inhibitor of the PLA_2 activity of Prdx6 (14).

We evaluated the effect of liposomal composition on protein binding using real-time fluorescence measurements of the interaction of bisPyr-PC-labeled liposomes with Prdx6. Binding by wild-type Prdx6 was similar for PG- and PS-containing liposomes, but binding by PE-containing liposomes was decreased markedly (Fig. 2C). Similar results were obtained using N-DNS-PE-labeled liposomes. The binding rate constant (k_1) for liposomes of different composition was calculated from the results obtained with N-DNS-PE-labeled liposomes (**Table 3**). Apparent k_1 for binding of wild-type Prdx6 was similar for the anionic PG- and PS-containing liposomes. Substitution of PG or PS with PE resulted in a ~50% decrease of apparent k_1. Because the size of liposomes was similar before and after incubation with Prdx6 (Table 1), the decreased k_1 indicates decreased Prdx6 binding, reflecting the effect of the liposomal surface charge. These results indicate the requirement of a negatively charged (anionic) phospholipid for maximal binding of Prdx6 to the liposomal surface, as described previously for secreted PLA_2 (22). The effect of liposome composition on the binding of Prdx6 also was studied by quenching of tryptophan fluorescence in the presence of increasing concentrations of NaI (Fig. 2D). The results are expressed as Stern-Völmer plots. The lesser decrease in I/Io of protein in solution by the addition of liposomes shows diminished accessibility of the tryptophanyl groups in Prdx6 for quenching. This effect was greatest for PG- or PS-containing liposomes and was blunted with PE-containing liposomes (Fig. 2D). This indicates that substitution of the uncharged phospholipid (PE) for anionic phospholipids (PG or PS) in unilamellar liposomes diminished Prdx6 binding.

The effect of mutations in Prdx6 on its binding to N-DNS-labeled liposomes was studied by real-time measurement of fluorescence. Unlike the wild-type protein, the S32A and H26A mutant proteins failed to show any change in fluorescence when incubated with liposomes (**Fig. 3A**), indicating that mutation of these residues abolished phospholipid binding. Binding of the D140A and W82F mutants to liposomes was similar to that of the wild type, whereas binding of the W33F mutant was 50% less. Except for the D140A mutant, the results for binding show good correspondence with PLA_2 activity (Table 2), compatible with the requirement of substrate binding for catalysis. The apparent k_1 for those mutant Prdx6 proteins that bound to the liposomes was calculated (Table 3).

To determine the K_d for binding of Prdx6 to liposomes, we used the equilibrium (saturation) values of the fluorescence ratio obtained with DNS-labeled liposomes for increasing concentrations of Prdx6 as a function of protein concentration (Fig. 3B). Figure 3B shows binding for wild-type and tryptophan mutant proteins to PG-containing liposomes and wild-type to PE-containing liposomes (Fig. 3B). The binding curve for the D140A mutant to PG-containing liposomes was similar to that of the wild type; no binding was observed for the S32A and H26A mutants (data not shown). The calculated apparent K_d values (Table 3) indicate strong binding of the wild-type protein to negatively charged (PG and PS) liposomes and

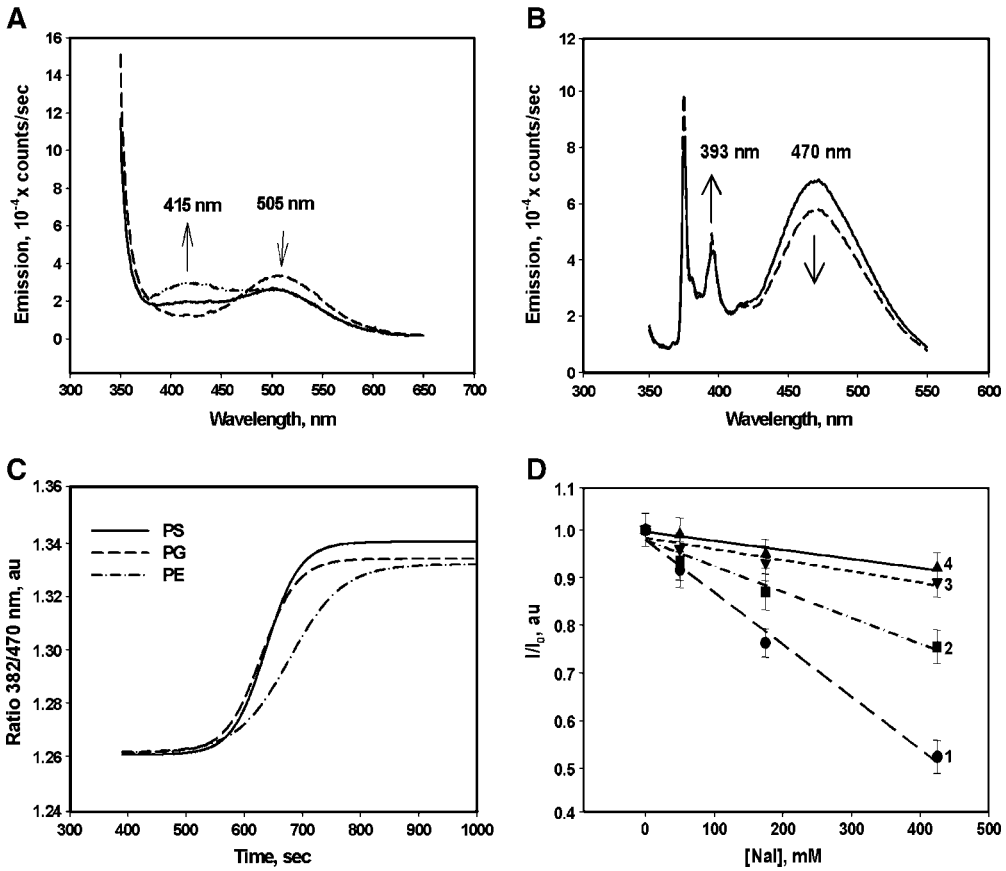

Fig. 2. Prdx6 binding to *N*-(5-dimethylaminonaphthalene-1-sulfonyl)-*sn*-glycero-3-phosphoethanolamine (N-DNS-PE)-labeled or 1,2-bis(1-pyrenedecanoyl)-*sn*-glycero-*3*-phosphocholine (bisPyr-PC)-labeled and unlabeled unilamellar liposomes. A: Hypsochromic shift of emission of N-DNS-PE-labeled liposomes (10 μM total lipid; dashed line) in 40 mM Na acetate buffer (pH 4.0) upon addition of 0.16 μM (solid line) or 0.32 μM (dotted and dashed line) wild-type Prdx6. N-DNS-PE was 2 mol% of total lipid. B: Increase in pyrene monomer fluorescence and decrease in excimer fluorescence upon addition of 0.32 μM wild-type Prdx6 (dashed line) to bisPyr-PC-labeled liposomes (10 μM total lipid; solid line). BisPyr-PC was 2 mol% of total phospholipid. C: Binding of wild-type Prdx6 determined with bisPyr-PC-labeled liposomes (100 μM total phospholipid) containing 10% phosphatidylglycerol (PG), phosphatidylserine (PS), or phosphatidylethanolamine (PE) in 40 mM Na acetate buffer, pH 4. Binding is shown in real time by detection of bisPyr-PC monomer to excimer ratio (382/470 nm). au, arbitrary units. D: Stern-Völmer plots for quenching of wild-type Prdx6 tryptophanyl fluorescence by increasing concentrations of NaI: line 1, Prdx6 (0.32 μM) in solution; line 2, Prdx6 plus PE-containing liposomes; line 3, Prdx6 plus PG-containing liposomes; line 4, Prdx6 plus PS-containing liposomes. Liposomes were added at 10 μM total lipid. Error bars indicate ± SEM. n = 3.

binding was significantly diminished with uncharged (PE) liposomes. The apparent K_d values for the D140A and W82F mutants were similar to the wild-type value, whereas the W33F mutant showed significantly increased K_d. In the absence of binding, K_d was not calculated for the S32A and H26A mutants.

The method for the measurement of K_d required the separation of bound and unbound Prdx6 by filtration, as described in Experimental Procedures. Western blot was used to evaluate the adequacy of separation under these conditions. Wild-type Prdx6 without liposomes showed ~90% of protein in the filtrate (**Fig. 4A**). With the addition of liposomes to Prdx6 at a concentration above the calculated apparent K_d, approximately equal amounts were recovered in the retentate and filtrate by protein fluorescence (Fig. 4B) and by PAGE (Fig. 4C). Dansyl fluorescence from lipid was detected only in the retentate, confirming that it contained the Prdx6-liposome complex (Fig. 4B). With Prdx6 at a concentration below the apparent K_d, no protein was present in the filtrate (Fig. 4C). With H26A mutant protein at a concentration above the apparent K_d, 88% of the protein was in the filtrate (Fig. 4D). These results validate the methodology used for the fluorescence analysis of protein binding.

Interaction of Prdx6 with N-DNS-PE and Pyr-PC probes

The addition of Prdx6 to N-DNS-PE micelles resulted in a decrease of protein tryptophanyl fluorescence and a subsequent increase of DNS fluorescence, indicative of FRET (**Fig. 5A**). FRET was substantially diminished when

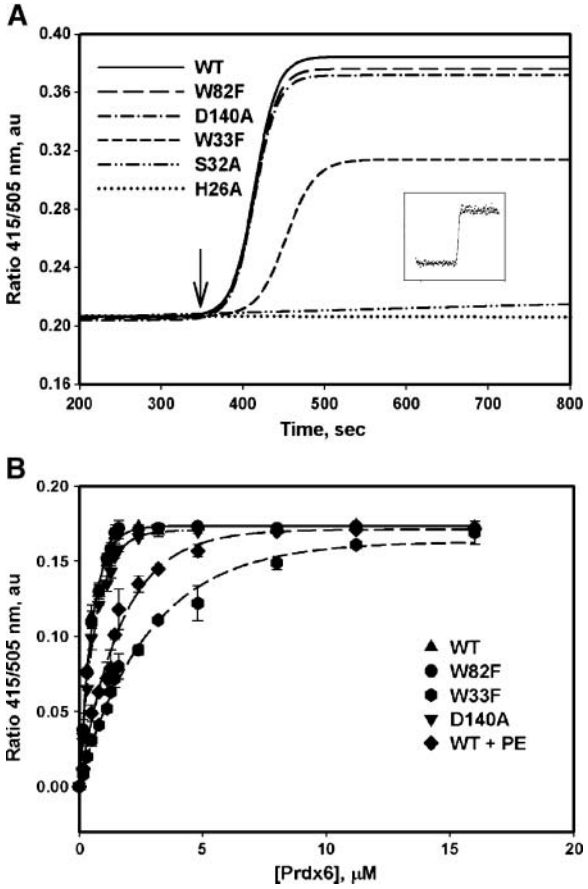

Fig. 3. Kinetics of binding of Prdx6 wild type and mutants to N-DNS-PE- or bisPyr-PC-labeled unilamellar liposomes. Liposomes (100 μM total phospholipid) were suspended in 40 mM Na acetate buffer, pH 4, and binding was determined by measurement of the fluorescence ratio (415/505 for N-DNS-PE or 382/470 for bisPyr-PC). All proteins were added (shown by the arrow) at a final concentration of 3.2 μM. Each curve is representative of three independent experiments. A: Binding determined with N-DNS-PE-labeled liposomes. Wild-type (WT) Prdx6, W82F, W33F, and D140A are shown using a sigmoid fit. S32A and H26A are shown using a linear fit. Liposomes had the standard composition, with PG as the anionic phospholipid. Binding is shown in real time by detection of the DNS fluorescence ratio (415/505 nm). The inset shows the individual data points for the wild type protein. B: Fluorescence ratio for N-DNS-PE-labeled unilamellar liposomes as a function of Prdx6 concentration. Studies with the wild type and D140A, W33F and W82F mutants used the standard (PG-containing) liposomes. WT + PE indicates wild-type Prdx6 with PE-containing liposomes. Values represent means ± SEM for three independent experiments. au, arbitrary units.

the W33F mutant was used instead of the wild-type protein, indicating that W33 is responsible for FRET associated with the phospholipid head group (Fig. 5A). The increase of DNS fluorescence attributable to FRET was small compared with the decrease of tryptophanyl fluorescence, which may reflect a difference in the orientation of W33 emission and DNS excitation dipoles. The position of the DNS emission maximum by FRET is ~480 nm, which is compatible with shielding of this chromophore from the surrounding medium as a consequence of binding. These

TABLE 3. Apparent rate constants measured for the binding of Prdx6 proteins to N-DNS-PE-labeled unilamellar liposomes

Protein	Liposome Composition[a]	Rate Constant	Dissociation Constant
		$10^6\ M^{-1}\ s^{-1}$	μM
Wild type	PG	11.3 ± 2.5	0.36 ± 0.11
Wild type	PS	10.0 ± 2.2	0.34 ± 0.10
Wild type	PE	5.5 ± 1.2	1.12 ± 0.19
S32A	PG, PE, or PS	ND	ND
H26A	PG, PE, or PS	ND	ND
D140A	PG	10.5 ± 1.8	0.45 ± 0.10
W82F	PG	10.3 ± 1.7	0.35 ± 0.11
W33F	PG	3.7 ± 0.8	2.12 ± 0.15

Data represent means ± SEM for three independent experiments. ND, no binding was detected.

[a] Liposomes contained (on a molar basis) 0.50 DPPC, 0.25 egg PC, 0.15 cholesterol, 0.10 of the indicated phospholipid, and 0.02 N-DNS-PE.

results indicate that W33 is in close proximity to the polar head of N-DNS-PE upon its binding to the surface of the protein globule.

The addition of Prdx6 to bisPyr-PC micelles resulted in a decrease of protein tryptophanyl fluorescence (~40%) and a subsequent increase of monomer fluorescence of the pyrene chromophore (Fig. 5B) associated with FRET. The results were similar after the substitution of bisPyr-PC with 2Pyr-PC (data not shown), indicating that the *sn*-2 acyl chain of these probes is responsible for FRET. This effect was significantly diminished by substitution of the W82F mutant for the wild-type protein, compatible with the close proximity of the *sn*-2 acyl chain of phospholipid to W82 upon its binding to Prdx6 (Fig. 5C). Fluorescence of the W82F mutant was significantly lower (~25%) than that of the wild type, indicating that W82 is largely responsible for protein fluorescence. These spectra were normalized to the maximal emission of the proteins without bisPyr-PC probe. To observe the effect of Prdx6 on absolute bisPyr-PC fluorescence, equimolar amounts of wild-type Prdx6 were incubated with bisPyr-PC micelles (Fig. 5D). There was a substantial increase (~70%) of monomer pyrene fluorescence at the expense of excimer fluorescence. This indicates the specific positioning of phospholipid substrate acyl chains, which prevents their contact to form an excimer, upon binding to Prdx6.

To study the stoichiometry of binding, bisPyr-PC micelles were treated with increasing concentrations of wild-type Prdx6 while recording both monomer and excimer fluorescence of the bisPyr-PC probe. The increase of monomer and decrease of excimer fluorescence showed saturation at a 1:1 (Prdx6/bisPyr-PC) molar ratio (Fig. 5E), indicating binding of one molecule of probe per molecule of Prdx6.

Effects of site-specific mutagenesis on Prdx6 secondary structure

The effect of the site-specific mutations on protein binding to liposomes raised the question of whether the structure of the protein had been altered. Wild-type and mutant proteins were analyzed by CD (**Fig. 6A**). Analysis by

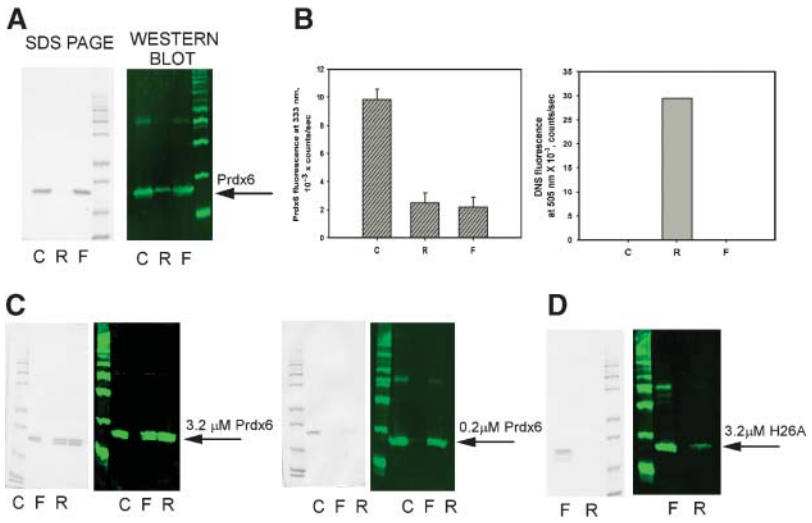

Fig. 4. SDS-PAGE, immunoblot, and fluorescence analysis of the binding of Prdx6 wild type and H26A mutant proteins to N-DNS-PE-labeled unilamellar liposomes. After incubation of protein with N-DNS-PE-labeled unilamellar liposomes (100 μM total lipid) at room temperature for 30 min, the sample was centrifuged to obtain retentate (R) and filtrate (F) as described in Experimental Procedures. Wild-type Prdx6 without liposomes was used as a control (C). A: Control incubation of wild-type protein in the absence of liposomes. B: Protein (left) and dansyl (right) fluorescence for filtrate and retentate after incubation of Prdx6 (3.2 μM) with liposomes. C: Incubation with wild-type Prdx6 at concentrations above (3.2 μM) and below (0.2 μM) the calculated dissociation constant (K_d). D: Incubation with H26A mutant protein at a concentration (3.2 μM) above the K_d. Error bars indicate ± SEM. n = 3.

the program K_{2d} showed essentially equal contributions of α-helix, β-strand, and random regions to the secondary structure of wild-type Prdx6. Mutation of S32 to alanine (S32A) or the neighboring W33 (W33F) resulted in substantial effects on secondary structure, with a marked increase in the content of α-helices and a decreased content of β-sheets (Fig. 6A). In contrast, the mutation of H26 (H26A), D140 (D140A), or W82 (W82F) had negligible effect on Prdx6 secondary structure. These data indicate the importance of both the β-turn at amino acids 30–32, which contains S32, and the β-strand at amino acids 33–40, which contains W33, for the secondary structure of Prdx6. Oxidation/reduction or mutation of C47 (C47S), the residue responsible for glutathione peroxidase activity in Prdx6, had no significant effect on the secondary structure of the protein (data not shown).

Effects of phospholipid substrate and MJ33 binding on Prdx6 secondary structure, melting temperature, and fluorescence

The addition of phospholipid substrate (micellar DPPC, as for the FRET analysis) resulted in minimal changes in the secondary structure (Fig. 6B) or melting point (Fig. 6C) of wild-type Prdx6 protein. The results (data not shown) for incubation with the unsaturated phospholipid substrate (PLPC) were the same as for DPPC. This result is consistent with the formation of a relatively stable enzyme-phospholipid substrate complex. On the other hand, the addition of the PLA_2 transition state inhibitor MJ33 resulted in a relatively small increase of α-helices in the Prdx6 secondary structure as well as a decrease in the slope of the protein melting curve at lower temperatures (40–60°C) (Fig. 6B, C). The difference in effects on secondary structure of Prdx6 between binding of DPPC or MJ33 may result from differences in their molecular composition, particularly the substitution of the *sn*-3 polar head group in the substrate by trifluoroethanol in the inhibitor. The MJ33 effect on the Prdx6 melting curve is compatible with its competitive inhibition of PLA_2 activity, indicating decreased stability of the Prdx6-MJ33 complex compared with the Prdx6-DPPC complex.

The addition of a 2× molar excess of MJ33 to Prdx6 resulted in an ~15% decrease of protein fluorescence (Fig. 6D). This quenching of tryptophanyl fluorescence indicates the binding of MJ33 to Prdx6. Quenching is most likely by the trifluoroethanol moiety of MJ33, compatible with the close proximity of this moiety to protein tryptophanyl(s). Quenching of fluorescence by MJ33 did not occur with the W33F mutant (data not shown), providing evidence that W33 is responsible for the quenched emission in the wild-type protein.

DISCUSSION

The PLA_2 activity of Prdx6 as well as its significance in lung surfactant catabolism have been extensively documented (5–8, 13–16). The activity is Ca^{2+}-independent and is maximal at pH 4. PC, the major phospholipid in lung surfactant, was shown to be the preferred substrate for the enzyme, whereas hydrolysis of PG, PS, and PE occurred with lesser efficiency (6, 7). The pioneering work of Jain and associates (23) demonstrated that the activity of secreted PLA_2 enzymes is a two-stage process that

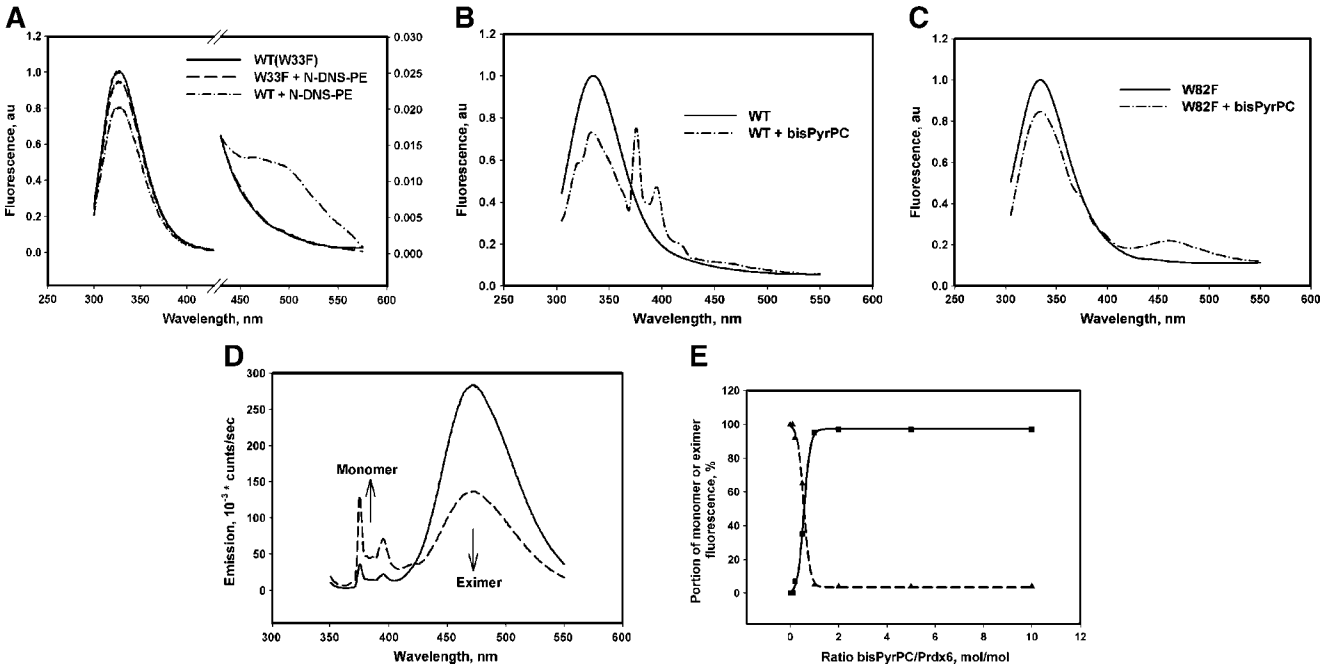

Fig. 5. Effects of Prdx6 binding on fluorescence resonance energy transfer (FRET) from Prdx6 to N-DNS-PE or bisPyr-PC probes. A: FRET from wild-type (WT) and W33F mutant proteins to the DNS chromophore before and after the addition of protein (0.5 μM) to micelles of N-DNS-PE (0.1 μM) in 40 mM Na acetate buffer, pH 4.0. Excitation was at 295 nm. The change of scale represents the amplified spectral area (400–600 nm) of DNS fluorescence. au, arbitrary units. B: FRET from wild-type and W82F mutant proteins to the pyrene chromophore before and after the addition of protein (0.5 μM) to micelles (0.1 μM) of bisPyr-PC. Excitation was at 295 nm. All spectra for FRET analysis were normalized to subsequent protein fluorescence without the addition of probes. C: Emission spectra (excitation at 340 nm) of bisPyr-PC micelles (0.1 μM) before (solid line) and after (dashed line) the addition of 0.2 μM wild-type Prdx6. D: Titration of bisPyr-PC micelles (0.1 μM) with wild-type Prdx6 (0–1 μM) with detection of monomer (solid line) and excimer (dashed line) fluorescence. Values represent the percentage of total fluorescence (excitation was at 340 nm). Spectra were recorded at 15 min after the addition of protein and incubation at 22°C. Spectra are representative of three independent experiments. E: Demonstration of the dependence of the monomer (solid line) and excimer (broken line) fluorescence on the bisPyr-PC to Prdx6 molar ratio. Saturation of the effect on fluoescence is seen at 1:1 molar ratio of lipid to protein.

involves binding of the enzyme to the vesicle surface followed by interfacial catalysis. Interfacial catalysis in turn involves binding of substrate to the active site followed by hydrolysis of the *sn*-2 ester bond. To better understand the mechanism for the PLA_2 activity of Prdx6, the present work focused on the structure-function relationships associated with these three steps: binding of protein to liposomes (representing an interfacial surface); substrate binding to the active site of the enzyme; and hydrolysis.

Binding of Prdx6 to the interfacial surface

Prdx6 binding to the interfacial surface was studied using liposomes of the same composition as used for our standard PLA_2 activity assay (50% DPPC, 25% egg PC, 15% cholesterol, and 10% PG). These liposomes mimic the composition of lung surfactant, the major physiological substrate for PLA_2 activity (5, 14–16). A fluorescent label was incorporated into the liposomes to serve as a reporter for Prdx6 binding. An increase in short-wavelength (~415 nm) fluorescence, presumably caused by the shielding of chromophore from the surrounding medium, indicated protein binding to N-DNS-PE-labeled liposomes. Similarly, Prdx6 binding to the surface of bisPyr-PC-labeled liposomes resulted in increased monomer fluorescence at the expense of the excimer fluorescence of the pyrene chromophore. These methods have been used in the past to study the polarity of the dansyl chromophore microenvironment as well as membrane fluidity changes (17, 24), and they were used in the present study to avoid a requirement to separate liposome-bound and free protein (25). The method is based on high quantum yields from dansyl and pyrene chromophores, the high sensitivity of the dansyl moiety to the polarity of its microenvironment, and the ability of pyrene to emit distinctive monomer and excimer fluorescence (20, 26). Thus, the fluorescence signals in both cases are proportional to the amount of bound Prdx6. The use of labeled liposomes should reflect the kinetics and thermodynamics of Prdx6 binding, because minimal amounts of probe (2 mol%) were used and the two probes have differentially localized chromophores: DNS at the liposome surface and Pyr close to the center of the bilayer (20). The results for bound and free Prdx6 using immunoblot and DNS fluorescence at concentrations of protein above and below the K_d show a good correlation with the determination of binding using fluorescence analysis. This supports the assumption that saturation of the fluores-

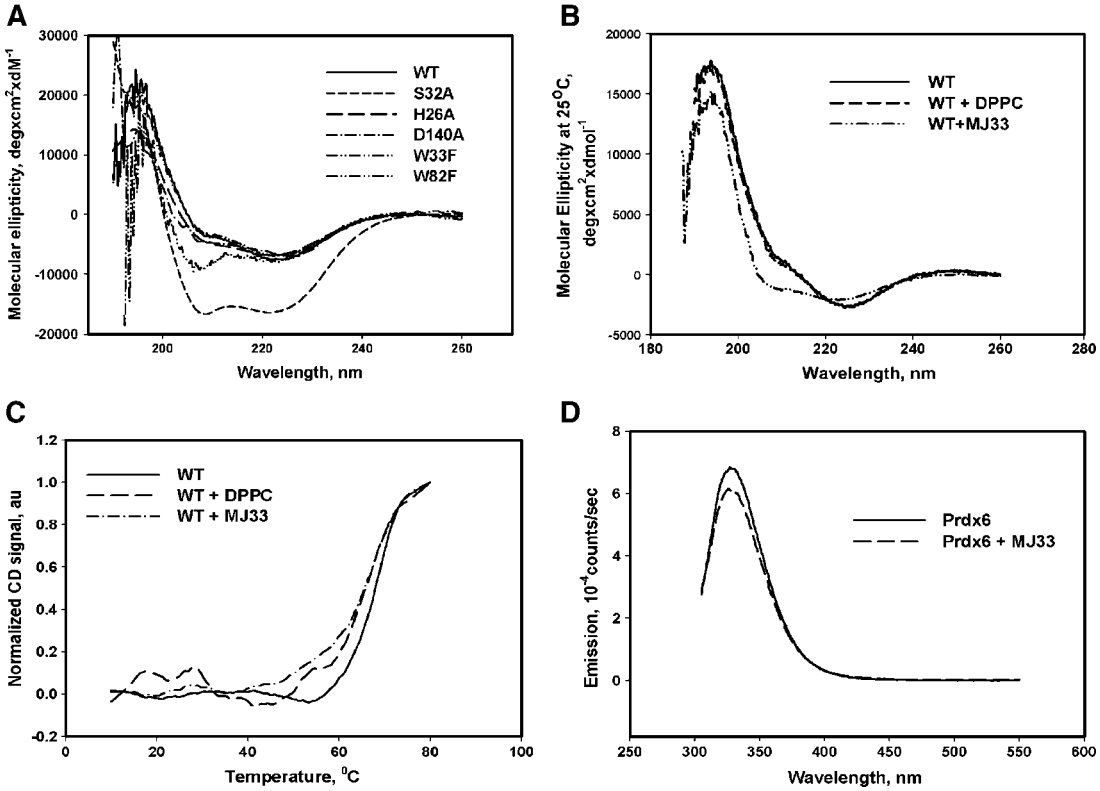

Fig. 6. Analysis of Prdx6 secondary structure by circular dichroism (CD) and tryptophanyl fluorescence. CD measurements were made at 25°C. A: CD spectra of wild-type (WT) Prdx6 and S32A, H26A, D140A, W33F, and W82F mutant proteins (50 μM) were measured in 40 mM Na acetate buffer, pH 4. B: The effect of phospholipid substrate [dipalmitoyl phosphatidylcholine (DPPC), 10 μM] and a transition state PLA_2 inhibitor (MJ33, 10 μM) on Prdx6 (50 μM) secondary structure. C: Melting curves for Prdx6 (50 μM) or complexes of Prdx6-DPPC or Prdx6-MJ33 (both at 50 μM). Melting curves were recorded as temperature dependence of molecular ellipticity at 220 nm. Each melting curve was normalized to its maximal CD signal, and the melting point was determined as the temperature at 50% loss of molecular ellipticity. au, arbitrary units. D: Fluorescence of wild-type Prdx6 (0.5 μM) before (solid line) and after (dashed line) the addition of 1 μM MJ33. Excitation was at 295 nm. Each spectrum is representative of three independent experiments.

cence signal corresponds with the apparent equilibrium between free protein and protein that is bound to liposomes. Quenching of Prdx6 tryptophanyl fluorescence using NaI shows protein binding to unlabeled liposomes, thus eliminating the possibility of any specific affinity of Prdx6 for the fluorescent probes.

Analysis of the binding kinetics for Prdx6 to liposomes allowed the calculation of an apparent k_1, whereas titration of fluorescently labeled liposomes with Prdx6 allowed the calculation of apparent K_d. This calculated value is an apparent K_d, because it presumably represents a two-step process of binding of enzyme to the vesicle surface followed by positioning of the phospholipid substrate at the enzyme active site. The results showed apparent $k_1 > 10.0 \times 10^6$ M^{-1} sec^{-1} and apparent $K_d \sim 0.36$ μM for both wild-type and W82 mutant Prdx6 titrated to negatively charged liposomes. These results indicate relatively fast and tight binding of Prdx6 to the interfacial surface. By comparison, the K_d for the interaction of cobra venom PLA_2 with dioleoyl PC vesicles is 0.6 μM (25).

The important effect of a negative liposomal surface charge on interfacial binding by secreted PLA_2 is well known (25). The present study provides similar results for Prdx6. The addition of PG with an apparent $Pk_a \sim 3.5$ (27) or PS with an intrinsic $Pk_a \sim 2.3$ for the carboxyl group (28) to liposomes provides a negative charge at pH 4. The calculated isoelectric point for Prdx6 is ~5.96 (http://www.embl-heidelberg.de/cgi/pi-wrapper.pl), consistent with experimentally determined values (29). Thus, Prdx6 will have a positive bulk charge at pH 4, facilitating the interaction with PG- or PS-containing liposomes. The estimated kinetic constants for Prdx6 binding to PG- or PS-containing liposomes were similar (Table 3). On the other hand, substitution of PG with PE results in a neutral charge of the liposomal surface, which was reflected in a significantly reduced apparent k_1 and increased apparent K_d. Thus, the presence of a negative charge on the liposome is as essential for tight binding as the initial step in Prdx6 catalysis.

Binding of phospholipid substrate to Prdx6

Our study of binding of phospholipid substrate to the active site of the enzyme was based upon an analysis of FRET from Prdx6 tryptophanyls to dansyl or pyrene chromophores contained in phospholipid probes. This

study used micelles of N-DNS-PE and bisPyr-PC to provide sufficient concentration of probe. N-DNS-PE is one of the most effective acceptors of protein tryptophanyl fluorescence. The dansyl chromophore contains the dimethylamino group, similar to that of choline in PC. It is likely that the bulky dansyl chromophore diminishes the effectiveness of N-DNS-PE binding to enzyme, which explains the relatively low FRET-induced fluorescence of acceptor as well as the relatively small shift of dansyl fluorescence from 505 to ~480 nm seen in the present studies. These effects may underlie the unsuccessful use of FRET with N-DNS-PE for K_d analysis in the past (25). FRET from Prdx6 to the dansyl chromophore was abolished by the W33F mutation, which indicates that W33 is the principal energy donor to N-DNS-PE. Because W33 is adjacent to S32, FRET indicates binding of the phospholipid polar head in proximity to S32 and provides evidence that S32 is indeed part of the PLA_2 catalytic triad.

BisPyr-PC was used to provide information about the positioning of the phospholipid acyl chains upon the binding of substrate to Prdx6. An increase in monomer at the expense of excimer during the incubation of Prdx6 with bisPyr-PC micelles indicates separation of the acyl chains upon binding of the bisPyr-PC probe. The W82 mutation abolished the increase in monomer fluorescence, indicating that this residue is the principal source of FRET to the pyrene monomer. W82 is inside the hydrophobic cleft of Prdx6 and is ~3.5 Å distant from the peroxidatic C47. Thus, FRET analysis using the two probes is compatible with binding of the phospholipid polar head to Prdx6 in the vicinity of the S32 moiety and of the *sn*-2 acyl chain in the vicinity of the peroxidatic C47. This specific positioning can explain the two catalytic functions of Prdx6: hydrolysis of phospholipid by the PLA_2 catalytic triad and reduction of the oxidized *sn*-2 acyl chain by the catalytic cysteine.

Effects of Prdx6 folding

The requirement of a serine in the active site of Prdx6 was demonstrated initially through inhibition of its PLA_2 activity by "serine protease" inhibitors such as diethyl nitrophenyl phosphate (6–8, 13, 30). Subsequently, loss of activity by the mutation of S32 suggested the importance of this amino acid residue in Prdx6 function (13). In the present study, we analyzed Prdx6 secondary structure to discriminate between structural and functional effects of the S32 mutation. Mutation of S32 resulted in a marked change in protein folding, leading to a helical structure and the elimination of the β-sheets that constitute the thioredoxin fold. Thus, S32 appears to have a crucial role in maintaining Prdx6 structure, and its mutation may affect PLA_2 activity secondarily. Of note, mutation of the catalytic serine in other serine-based PLA_2s did not alter protein folding (31), indicating that Prdx6 might be unique in that regard.

Mutation of the other components of the putative catalytic triad (H26 and D140) had no measurable effect on secondary structure. Mutation of W33, adjacent to S32, increased the α-helical content of Prdx6 and resulted in an ~50% inhibition of PLA_2 activity. In comparison, the secondary structure of the W82 mutant as well as its PLA_2 activity were similar to those of the wild-type protein. The substitution of W33 by phenylalanine would change the apparent hydrophobicity (derived as the mean fractional accessibility of tryptophan and phenylalanine in an average protein structure) minimally from 0.87 to 0.88 but would result in a substantial change in the surface area from 266.8 to 222.8 $Å^2$ (32). Approximation of this area as a circle yields an ~0.8 Å difference in radius, indicating precise alignment of W33 and presumably S32 in the vicinity of the PLA_2 catalytic triad.

The addition of phospholipid (DPPC or PLPC) micelles to Prdx6 also did not affect protein folding as analyzed by CD. However, the addition of MJ33, a PLA_2 competitive transition state analog, resulted in an increase of α-helical content in Prdx6. MJ33 differs from substrate phospholipids in that its polar head is substituted by phosphomethanol and the *sn*-2 acyl chain is substituted by a trifluoroethyl moiety. The slight distortion of Prdx6 folding by MJ33 could reflect the repulsion of its phosphate by the D31 residue in the β-turn. A similar result was shown for the complex of MJ33 with bovine pancreatic PLA_2 (33). Thus, the site of binding to Prdx6 for the phosphomethanol moiety of MJ33 corresponds to the vicinity for binding to substrate, providing a mechanism for its effectiveness as an inhibitor of the PLA_2 activity of this protein (13–16). Support for this finding came from the analysis of Prdx6 melting temperature. DPPC, PLPC, and MJ33 binding by Prdx6 resulted in the same shift of melting temperature of enzyme from 69°C for free enzyme to 65°C for enzyme bound to substrate/inhibitor. As an additional support, mutation of W33 abolished the quenching of Prdx6 fluorescence by MJ33 that was observed with wild-type protein.

Catalytic center for PLA_2 activity

Although the S32A mutation studies are inconclusive, additional evidence supports the role of S32 as a component of the catalytic triad. First, S32 is part of the lipase motif (GXSXG) that has been found in serine-based lipases (9, 30, 34), and this motif does not occur elsewhere in Prdx6 (6–8). Second, analysis of the tertiary (crystal) structure of the protein (Fig. 1) indicates that S32 is positioned appropriately on the surface to function in substrate (lipid) binding and is also positioned appropriately to interact with H26-D140 for catalysis. Third, this postulated positioning of S32 is supported by the experiments showing FRET from the adjacent W33, indicating the binding of phospholipid substrate. Distinct from the effects of S32 and W33 mutations, mutation of H26A or D140A had essentially no effect on Prdx6 secondary structure. However, mutation of H26 did abolish binding to liposomes, indicating that it is sited at the binding interface; because its mutation abolishes binding, its role in catalysis cannot be confirmed by this approach. On the other hand, the D140 mutation had no effect on lipid

binding, but PLA_2 activity of Prdx6 was abolished, compatible with a role for this residue in catalysis.

Conclusions

The results presented in this study indicate tight binding of Prdx6 to the negatively charged phospholipid bilayer, which corresponds with the "scooting" mode of interfacial catalysis proposed for other PLA_2 enzymes (22, 23, 25). Furthermore, these studies are consistent with the hypothesis that S32, H26, and D140 function as a catalytic triad. This triad is commonly found in other serine-based lipases (12, 34–36). Mutation of the individual members of the proposed triad results in loss of the PLA_2 activity of Prdx6, although the effect of each appears to be through a different mechanism. Mutation of S32 results in alterations of protein structure and loss of its ability to bind to the liposome interface. Mutation of H26 also results in the loss of interfacial binding, although in this case the protein structure is maintained. Thus, the surface of the protein in the area of H26 through W33 appears to be crucial for binding of the protein to the interface. Furthermore, the vicinity of S32 (namely the lipase motif) appears to be crucial for binding of the phospholipid polar head, which results in specific positioning of the substrate *sn*-2 ester bond and generates the conformation of enzyme necessary to perform hydrolysis. Mutation of D140 has no effect on the binding of substrate but abolishes catalysis. Finally, functional inactivation of Prdx6 peroxidase activity (via overoxidation of C47) does not affect its PLA_2 activity, indicating a clear distinction between the peroxidatic and hydrolytic sites of catalysis.

The authors thank Dr. Mahendra Jain for encouragement and advice, Dr. Walter Englander, Dr. Leland Mane, and Sabrina Bédard for their assistance in CD analysis, Dr. David Speicher for mass spectroscopy, Chandra Dodia for PLA_2 assay, Dr. Sergei Zaitsev for assistance with protein expression, Jonathan Held for assistance with figures, and Jennifer Rossi and Susan Turbitt for typing the manuscript. This work was supported by National Institutes of Health Grant HL-19737.

REFERENCES

1. Hofmann, B., H. J. Hecht, and L. Flohe. 2002. Peroxiredoxins. *Biol. Chem.* **383:** 347–364.
2. Rhee, S. G., S. W. Kang, T. S. Chang, W. Jeong, and K. Kim. 2001. Peroxiredoxin, a novel family of peroxidases. *IUBMB Life.* **52:** 35–41.
3. Wood, Z. A., E. Schroder, J. R. Harris, and L. B. Poole. 2003. Structure, mechanism and regulation of peroxiredoxins. *Trends Biochem. Sci.* **28:** 32–40.
4. Manevich, Y., S. I. Feinstein, and A. B. Fisher. 2004. Activation of the antioxidant enzyme 1-CYS peroxiredoxin requires glutathionylation mediated by heterodimerization with pi GST. *Proc. Natl. Acad. Sci. USA.* **101:** 3780–3785.
5. Fisher, A. B., C. Dodia, S. I. Feinstein, and Y. S. Ho. 2005. Altered lung phospholipid metabolism in mice with targeted deletion of lysosomal-type phospholipase A2. *J. Lipid Res.* **46:** 1248–1256.
6. Kim, T. S., C. S. Sundaresh, S. I. Feinstein, C. Dodia, W. R. Skach, M. K. Jain, T. Nagase, N. Seki, K. Ishikawa, N. Nomura, et al. 1997. Identification of a human cDNA clone for lysosomal type Ca^{2+}-independent phospholipase A2 and properties of the expressed protein. *J. Biol. Chem.* **272:** 2542–2550.
7. Akiba, S., C. Dodia, X. Chen, and A. B. Fisher. 1998. Characterization of acidic Ca(2+)-independent phospholipase A2 of bovine lung. *Comp. Biochem. Physiol. B Biochem. Mol. Biol.* **120:** 393–404.
8. Kim, T. S., C. Dodia, X. Chen, B. B. Hennigan, M. Jain, S. I. Feinstein, and A. B. Fisher. 1998. Cloning and expression of rat lung acidic Ca(2+)-independent PLA2 and its organ distribution. *Am. J. Physiol.* **274:** L750–L761.
9. Bhanot, P., K. Schauer, I. Coppens, and V. Nussenzweig. 2005. A surface phospholipase is involved in the migration of *Plasmodium sporozoites* through cells. *J. Biol. Chem.* **280:** 6752–6760.
10. Manevich, Y., and A. B. Fisher. 2005. Peroxiredoxin 6, a 1-Cys peroxiredoxin, functions in antioxidant defense and lung phospholipid metabolism. *Free Radic. Biol. Med.* **38:** 1422–1432.
11. Choi, H. J., S. W. Kang, C. H. Yang, S. G. Rhee, and S. E. Ryu. 1998. Crystal structure of a novel human peroxidase enzyme at 2.0 A resolution. *Nat. Struct. Biol.* **5:** 400–406.
12. Brady, L., A. M. Brzozowski, Z. S. Derewenda, E. Dodson, G. Dodson, S. Tolley, J. P. Turkenburg, L. Christiansen, B. Huge-Jensen, L. Norskov, et al. 1990. A serine protease triad forms the catalytic centre of a triacylglycerol lipase. *Nature.* **343:** 767–770.
13. Chen, J. W., C. Dodia, S. I. Feinstein, M. K. Jain, and A. B. Fisher. 2000. 1-Cys peroxiredoxin, a bifunctional enzyme with glutathione peroxidase and phospholipase A2 activities. *J. Biol. Chem.* **275:** 28421–28427.
14. Fisher, A. B., and C. Dodia. 1996. Role of phospholipase A2 enzymes in degradation of dipalmitoylphosphatidylcholine by granular pneumocytes. *J. Lipid Res.* **37:** 1057–1064.
15. Fisher, A. B., and C. Dodia. 2001. Lysosomal-type PLA2 and turnover of alveolar DPPC. *Am. J. Physiol. Lung Cell. Mol. Physiol.* **280:** L748–L754.
16. Fisher, A. B., C. Dodia, A. Chander, and M. Jain. 1992. A competitive inhibitor of phospholipase A2 decreases surfactant phosphatidylcholine degradation by the rat lung. *Biochem. J.* **288:** 407–411.
17. Fischkoff, S., and J. M. Vanderkooi. 1975. Oxygen diffusion in biological and artificial membranes determined by the fluorochrome pyrene. *J. Gen. Physiol.* **65:** 663–676.
18. Hagel, L., and T. Anderson. 1992. Size exclusion chromatography. In Chromatography. E. Hoffman, editor. Elsevier, North Holland, Amsterdam, The Netherlands. A267–A307.
19. Kucerka, N., M. A. Kiselev, and P. Balgavy. 2004. Determination of bilayer thickness and lipid surface area in unilamellar dimyristoylphosphatidylcholine vesicles from small-angle neutron scattering curves: a comparison of evaluation methods. *Eur. Biophys. J.* **33:** 328–334.
20. Lakowicz, J. R. 1999. Principles of Fluorescence Spectroscopy. Academic/Plenum, New York.
21. Wu, Y-Z., Y. Manevich, J. L. Baldwin, C. Dodia, K. Yu, S. I. Feinstein, and A. B. Fisher. 2006. Interaction of surfactant protein A with peroxiredoxin 6 regulates phopholipase A2 activity. *J. Biol. Chem.* **281:** 7517–7525.
22. Ghomashchi, F., B. Z. Yu, O. Berg, M. K. Jain, and M. H. Gelb. 1991. Interfacial catalysis by phospholipase A2: substrate specificity in vesicles. *Biochemistry.* **30:** 7318–7329.
23. Jain, M. K., M. H. Gelb, J. Rogers, and O. G. Berg. 1995. Kinetic basis for interfacial catalysis by phospholipase A2. *Methods Enzymol.* **249:** 567–614.
24. Plasencia, I., A. Cruz, C. Casals, and J. Perez-Gil. 2001. Superficial disposition of the N-terminal region of the surfactant protein SP-C and the absence of specific SP-B-SP-C interactions in phospholipid bilayers. *Biochem. J.* **359:** 651–659.
25. Berg, O. G., M. H. Gelb, M. D. Tsai, and M. K. Jain. 2001. Interfacial enzymology: the secreted phospholipase A(2)-paradigm. *Chem. Rev.* **101:** 2613–2654.
26. Wolf, D. E. 1988. Spectroscopic Membrane Probes. CRC Press, Boca Raton, FL.
27. Stewart, L. C., M. Kates, and I. C. Smith. 1988. Synthesis and characterization of deoxy analogues of diphytanylglycerol phospholipids. *Chem. Phys. Lipids.* **48:** 177–188.
28. Moncelli, M. R., L. Becucci, and R. Guidelli. 1994. The intrinsic pKa values for phosphatidylcholine, phosphatidylethanolamine, and phosphatidylserine in monolayers deposited on mercury electrodes. *Biophys. J.* **66:** 1969–1980.
29. Wattiez, R., I. Noel-Georis, C. Cruyt, F. Broeckaert, A. Bernard, and P. Falmagne. 2003. Susceptibility to oxidative stress: proteomic analysis of bronchoalveolar lavage from ozone-sensitive and ozone-resistant strains of mice. *Proteomics.* **3:** 658–665.
30. Tew, D. G., C. Southan, S. Q. Rice, M. P. Lawrence, H. Li, H. F.

Boyd, K. Moores, I. S. Gloger, and C. H. Macphee. 1996. Purification, properties, sequencing, and cloning of a lipoprotein-associated, serine-dependent phospholipase involved in the oxidative modification of low-density lipoproteins. *Arterioscler. Thromb. Vasc. Biol.* **16:** 591–599.
31. Patricelli, M. P., M. A. Lovato, and B. F. Cravatt. 1999. Chemical and mutagenic investigations of fatty acid amide hydrolase: evidence for a family of serine hydrolases with distinct catalytic properties. *Biochemistry.* **38:** 9804–9812.
32. Lesser, G. J., and G. D. Rose. 1990. Hydrophobicity of amino acid subgroups in proteins. *Proteins.* **8:** 6–13.
33. Sekar, K., S. Eswaramoorthy, M. K. Jain, and M. Sundaralingam. 1997. Crystal structure of the complex of bovine pancreatic phospholipase A2 with the inhibitor 1-hexadecyl-3-(trifluoroethyl)-sn-glycero-2-phosphomethanol. *Biochemistry.* **36:** 14186–14191.
34. Lowe, M. E. 1997. Structure and function of pancreatic lipase and colipase. *Annu. Rev. Nutr.* **17:** 141–158.
35. Schrag, J. D., Y. G. Li, S. Wu, and M. Cygler. 1991. Ser-His-Glu triad forms the catalytic site of the lipase from *Geotrichum candidum*. *Nature.* **351:** 761–764.
36. Wangikar, P. P., A. V. Tendulkar, S. Ramya, D. N. Mali, and S. Sarawagi. 2003. Functional sites in protein families uncovered via an objective and automated graph theoretic approach. *J. Mol. Biol.* **326:** 955–978.